https://doi.org/10.5194/egusphere-2025-6293
Preprint. Discussion started: 23 January 2026

Seasonal glacier motion variations and underlying hydro-mechanical processes at the Argentiere Glacier, French Alps

Anuar Togaibekov[1,2], Adrien Gilbert[1], Florent Gimbert[1], and Andrea Walpersdorf[2]

[1]IGE, Univ. Grenoble Alpes, CNRS, INRAE, IRD, Grenoble INP, 38000 Grenoble, France
[2]ISTerre, Univ. Grenoble Alpes, CNRS, IRD, UGE, 38000 Grenoble, France

Correspondence: Anuar Togaibekov (a.togaibekov@gmail.com)

Abstract. Subglacial hydrology controls basal sliding of hard-bedded glaciers by modulating basal drag through changes in ice–bed separation. Yet, the underlying mechanisms that control ice–bed separation and its links with basal friction remain poorly understood. In this study, we contribute to a better understanding of this problem by evaluating spatial and temporal changes in bed separation in relation to changes in glacier horizontal velocity using three years of continuous and dense GPS records from Glacier d'Argentière (French Alps). We confirm a previous study showing that spatial and temporal variations in glacier vertical motion mainly reflect changes in ice–bed separation, as they cannot be explained by variations in internal strain rates. We find that the ice–bed separation velocity is anti-correlated with subglacial water discharge, being positive in winter in the absence of surface melt and negative during summer melt. We suggest that this behavior results from basal cavities being weakly connected in winter, allowing them to fill slowly under low water input from englacial storage release or basal melt, and then rapidly transitioning to a connected state in summer, enabling efficient drainage of surface meltwater and reduced cavity sizes. Interestingly, changes in horizontal velocity are well correlated, both in time and space, with changes in ice–bed separation and can be quantitatively compared with modeled values related to subsequent variations in basal cavity size. These observational findings contrast strongly with previous observations in steeper parts of Glacier d'Argentière, where seasonal motion was positively correlated with subglacial water discharge and was argued to be primarily controlled by cavities being connected year-round. We discuss the potential mechanisms underlying these discrepancies and how they may also explain observations of seasonal glacier dynamics in Greenland.

1 Introduction

Glacier basal sliding generally exhibits seasonal variations, with summer speeds reaching up to three times the average speed in winter (Nienow et al., 1998; Ryser et al., 2014; Vincent and Moreau, 2016). These variations are controlled by the seasonal influx of surface meltwater beneath the glacier through moulins and crevasses, leading to the formation of various types of subglacial drainage systems (Iken and Bindschadler, 1986; Gordon et al., 1998; Mair et al., 2001; Harper et al., 2005), thought to consist of a combination of distributed (inefficient) and channelized (efficient) hydrological systems (Davison et al., 2019). Distributed systems are characterized by a widespread network of cavities (pockets between bedrock bumps) with varying degrees of connectivity and drainage efficiency, and are thought to dominate where and when water input rates are

https://doi.org/10.5194/egusphere-2025-6293
Preprint. Discussion started: 23 January 2026

low (Lliboutry, 1968; Fowler, 1987; Kamb, 1987; Andrews et al., 2014). In contrast, channelized systems consist of discrete channels that can incise into the ice through turbulence-induced melting (Röthlisberger, 1972), and are thought to form where and when meltwater input rates are high (Kamb, 1970; Fountain and Walder, 1998; Schoof, 2010; Hewitt et al., 2012; Werder et al., 2013). An intermediate situation in which cavities connect through small channels (orifices) may also exist (Kamb, 1970). However, the dominant type of hydrological system beneath a glacier and its relationship with overall basal sliding remain largely uncertain (Rada and Schoof, 2018).

Our current understanding of the physics of hard-bedded glacier basal sliding is mainly based on the seminal work of Weertman (1957) and Lliboutry (1958), sometimes referred to as "Weertman's Sliding Law" and "Lliboutry's Sliding Law," respectively (Gimbert et al., 2021a). In Weertman's Sliding Law, where the sliding velocity U_b is a function of basal drag τ_b only ($U_b = f(\tau_b)$), the ice-bed contact is assumed to be frictionless, and basal resistance instead arises at the meso-scale (from centimeters to a few tens of meters) due to ice flowing around bedrock irregularities from enhanced creep and pressure melting mechanisms (Weertman, 1957). This resistance is described by a friction coefficient A_s. Thanks to its simplicity, this law is widely used in modeling ice-sheet dynamics and associated future sea-level rise projections (Ritz et al., 2015). In contrast, Lliboutry's Sliding Law is more complex but more observationally motivated, as it introduces a dependence on effective pressure N at the ice-bed interface, with $U_b = f(N, \tau_b)$, where N is defined as the difference between the ice overburden pressure p_i and the subglacial water pressure p_w. Increased basal water pressure p_w reduces N and provides partial support for the weight of the glacier, increasing cavity size (also known as bed separation), reducing the apparent bed roughness, and thus enhancing basal sliding (Lliboutry, 1958; Hodge, 1974; Iken and Bindschadler, 1986; Fowler, 1987; Gagliardini et al., 2007). Lliboutry's formulation is also consistent with theoretical and experimental findings that basal shear stresses should be bounded (Iken, 1981; Schoof, 2005; Zoet and Iverson, 2020). Although it is well known that effective pressure governs basal friction, yet the processes that cause effective pressure to fluctuate are still not fully understood (Rada and Schoof, 2018).

The magnitude of the effective pressure N is controlled by the combined effect of the rate of meltwater supply and the transmissivity of the subglacial drainage, both of which are highly variable over a year (Iken et al., 1983; Iken and Bindschadler, 1986; Rada and Schoof, 2018; Gilbert et al., 2022). The development of the subglacial drainage system has long been recognized to start concurrently with the onset of the melting season (Iken and Bindschadler, 1986; Raymond et al., 1995; Vincent and Moreau, 2016). At this time of year, the distributed drainage system, which is likely represented by either a weakly connected or isolated network of cavities (Hoffman et al., 2016; Bartholomaus et al., 2011), transmits water at relatively slow speeds and builds up water pressure from the seasonal increase in meltwater input, resulting in a "spring acceleration" observed in many glaciers (Iken, 1981; Mair et al., 2001; Anderson et al., 2004; Bingham et al., 2008). As the melt season progresses, the distributed subglacial drainage system evolves into a channelized network capable of efficiently evacuating large volumes of meltwater through subglacial conduits at low water pressure, such that a glacier slows down (Röthlisberger, 1972). Recent borehole measurements have shown that both distributed and channelized subglacial drainage systems can co-evolve and exhibit strong spatial heterogeneity (Rada and Schoof, 2018). Because sliding velocity cannot be measured directly and borehole records capture only point-scale conditions, our understanding of the physical relationship between sliding velocity and effective pressure remains limited.

https://doi.org/10.5194/egusphere-2025-6293
Preprint. Discussion started: 23 January 2026

Glacier d'Argentière in the French Alps is one of the few glaciers where sliding velocity has been directly measured in a natural subglacial cavity at the terminus of the glacier (Vincent and Moreau, 2016). Using these long-term direct measurements, previous studies demonstrated that bed shear stress strongly influences effective pressure through a feedback between subglacial drainage and basal sliding (Gimbert et al., 2021a), and subsequently developed a fully coupled hydro-mechanical model to describe this interaction (Gilbert et al., 2022). However, a few hundred meters upstream, Vincent et al. (2022) observed winter uplift and acceleration, which they suggested may result from increasing bed separation due to the growth of basal cavities that remain isolated during winter. This discrepancy indicates that, beyond meltwater input, other factors such as ice thickness, surface slope, and bed topography may also modulate effective pressure.

Here we investigate subglacial hydrology and its influence on basal friction at the same site studied by Vincent et al. (2022), aiming to show that the seasonal pattern of hydrological variations and their control on friction differs, indicating that the underlying subglacial processes are also different, and we discuss potential mechanisms that could explain these discrepancies. To do so we use high resolution surface elevation and velocity observations obtained from a dense network of GPS stations, continuously operating for 3 years (2019–2021) in the ablation zone of the Glacier d'Argentière. From combined analysis of vertical and horizontal velocities, we reconstruct the evolution of basal cavity growth and sliding velocity, respectively, and interpret their respective variations in terms of changing subglacial hydrology and its control on basal friction. These unique observations contribute to a better understanding of the seasonal processes that control frictional changes as a function of the evolution of subglacial hydrology.

2 Data and methods

2.1 Study site

Glacier d'Argentière is located in the Mont-Blanc Massif in the French Alps (Fig. 1a) and is considered to be a hard-bedded glacier (Vivian and Bocquet, 1973; Gimbert et al., 2021a, b). It originates at about 3400 m a.s.l. and terminates at around 1600 m a.s.l., spanning a total length of ∼10 km. The equilibrium-line altitude laid at about 2900 m during 2019–2021 (Vincent et al., 2009). Our study site is located in the ablation zone at ∼2380 m, where the glacier is characterized by a sharply incised V-shaped valley (Hantz and Lliboutry, 1983; Vincent et al., 2009) and where previous studies have documented ice dynamics in relation to subglacial hydrology (Vincent et al., 2022; Togaibekov et al., 2024; Roldán-Blasco et al., 2024; Nanni et al., 2020, 2021). At this location, the glacier has a relatively shallow surface slope (10 %), a maximum thickness of 255 m (Fig. 1a), and an average melt rate from May to September of 0.06 m d^{-1} (Togaibekov et al., 2025).

2.2 Field set-up

Five Global Positioning System (GPS) stations were deployed in the ablation zone of Glacier d'Argentière in February 2019, with an additional seven stations installed in February 2020 (inset map in Fig. 1a). GPS antennas are mounted on aluminum poles anchored up to 6 m deep in the ice (Fig. 1b). The distance between neighboring survey stations ranges from 50 to

https://doi.org/10.5194/egusphere-2025-6293
Preprint. Discussion started: 23 January 2026

200 m. Regular field visits (monthly at most during a melting season) ensured the upright position of the antenna poles and continuous power supply. We employ multi-frequency Leica GR25 receivers and Leica AS10 antennas, which continuously record GPS signals at a 1 Hz sampling interval. The raw GPS data are decimated to 30-second intervals and converted into 24-hour-long RINEX (Receiver INdependent EXchange) format files. Although we collected multi-GNSS (Global Navigation Satellite Systems) observables, only GPS data were used in this study.

In addition to GPS, we utilize a wide range of complementary observations. In situ measurements of basal sliding velocity are made thanks to direct access to a subglacial cavity and the installation of specialized equipment known as a "cavitometer" (green diamond in Fig. 1a) (Gimbert et al., 2021a; Gilbert et al., 2022; Vincent and Moreau, 2016; Vivian and Bocquet, 1973). This equipment consists of a bicycle wheel (Fig. 1c) recording basal velocity at 30-minute intervals with a precision better than ± 1 cm d^{-1} (Vincent and Moreau, 2016). The glacier is steep and thin at the wheel location, whereas it is flatter and thicker at the GPS network site.

Water discharge (blue square in Fig. 1a) is recorded in excavated tunnels beneath the glacier tongue, a few hundred meters downstream of the cavitometer, at 15-minute intervals, with a discharge threshold of approximately 10 m^3 s^{-1} due to collector capacity limitations (Vincent and Moreau, 2016). This limitation was eliminated after an upgrade to a more advanced measurement device in summer 2020. The meltwater predominantly exits through a well-identified notch in the bedrock valley, with only a minimal amount of water flowing out elsewhere. Water pressure is measured in a borehole (yellow star in Fig. 1a) next to the GPS site ARG1 using a piezometer positioned 95 m above the bed. To obtain the basal water pressure, we add a constant pressure equivalent to the water column height of 95 m. The borehole was operational from September 2019 to October 2020, although it is thought that it decoupled from the subglacial hydraulic system during the summer of 2020 (Roldán-Blasco et al., 2024). We also use air temperature data obtained at 30-minute intervals from the SAFRAN meteorological reanalysis in the French Alps (Vernay et al., 2022).

2.3 GPS data processing

GPS data are processed in static mode with a double difference processing technique and ionosphere-free linear combination (LC) phase observables (Bock et al., 1986), incorportaed in the geodetic software package GAMIT/GLOBK (Herring et al., 2018). Daily GPS phase measurements are processed relative to well-determined 13 IGS (International GNSS Service) stations located at distances ranging from 110 km to 1080 km from Glacier d'Argentière. We empirically assess the quality of position estimates using the site ARGB on bedrock close to the survey network which is exposed to a similar multi-path scattering environment as the sites on the glacier (red triangle in Fig. 1a). This is because the formal errors generated by the software for a static position estimate are only applicable to "true" stationary sites; however, Glacier d'Argentière moves over 10 cm d^{-1}. Applying these formal errors would violate the least-squares requirement, resulting in overestimated and biased residuals (King, 2004). The position time series of the stationary site ARGB yields an average root-mean-square (RMS) of ± 2.1 mm and ± 6.1 mm for horizontal and vertical position estimates, respectively (Fig. S1a-c).

The daily position estimates are converted into horizontal and vertical velocity time series by subtracting successive coordinates over a 24-hour interval and dividing by this time interval. The velocity error at site ARGB is ± 2.3 mm d^{-1} (Fig. S1d), which

https://doi.org/10.5194/egusphere-2025-6293
Preprint. Discussion started: 23 January 2026

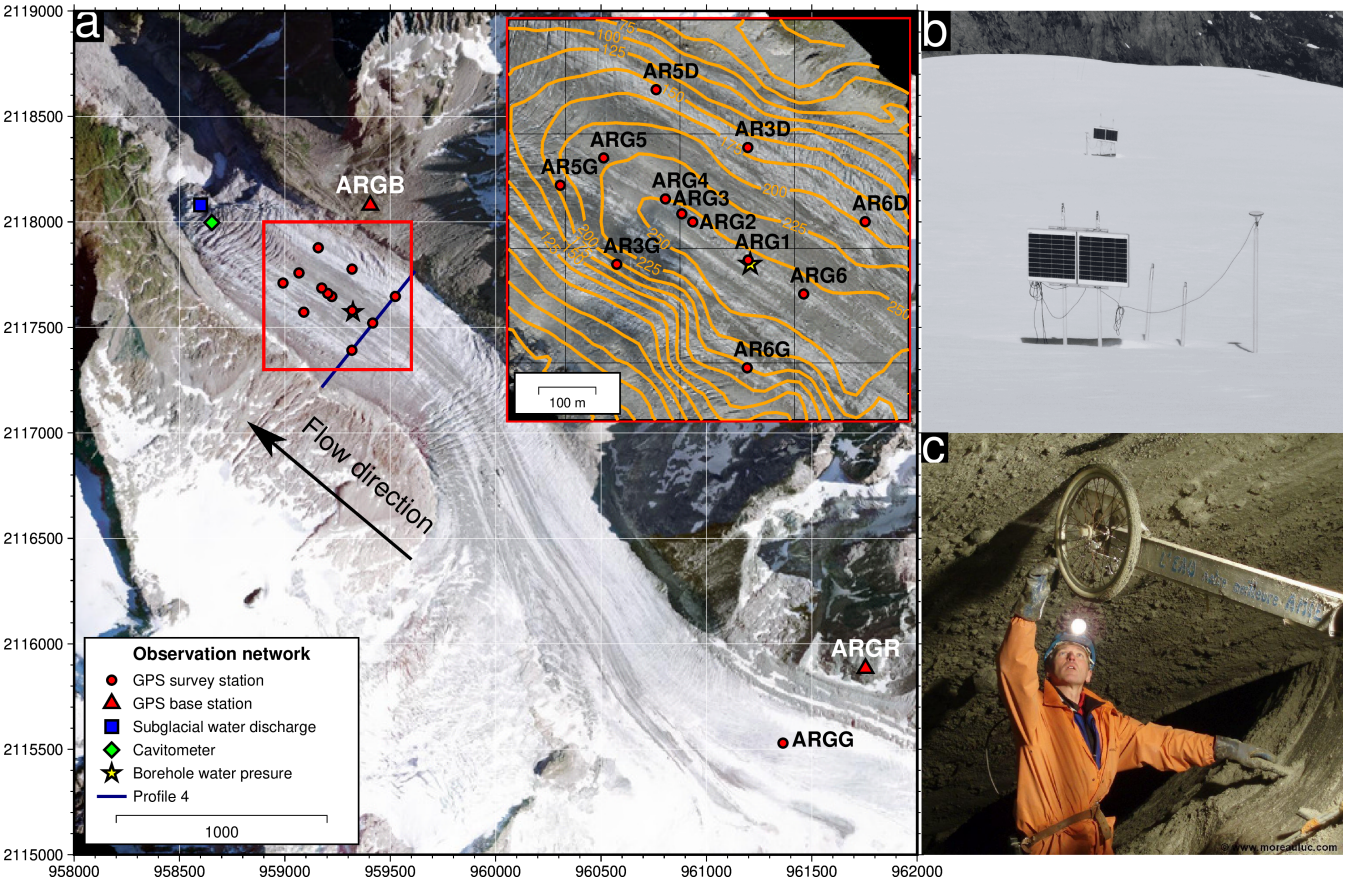

Figure 1. (a) Map showing the observation network at Glacier d'Argentière. The red rectangle indicates the location of twelve along-flow GPS sites (red circles, also shown in the top-right inset map). The dark blue line represents Profile 4, which was used to set the model parameters. The isolines in the inset show the glacier thickness in meters. Coordinates are given in the cartesian NTF (Paris)/Lambert zone II coordinate system. (b,c) Pictures of (b) two GPS stations and (c) the cavitometer.

we adopt for the survey stations on the glacier. Assuming the cyclic behavior of bed separation at the study site (Vincent et al., 2022), we remove a bed geometry-controlled linear trend in the vertical displacement time series for each annual cycle independently, ensuring that bed uplift returns to the same value each year. This approach imposes a common reference at an arbitrary datum, where the minimum point is set to zero. The mean values of the GPS-derived observables (horizontal velocity, vertical displacement, and vertical velocity) averaged across all sites are presented in Fig. 2. Time series of horizontal velocity and bed-separation-induced vertical displacement for individual GPS sites are provided in Supporting Information S1 (Fig. S2).

https://doi.org/10.5194/egusphere-2025-6293
Preprint. Discussion started: 23 January 2026

2.4 Model Description

The multidecadal measurements of basal sliding velocity and water discharge on Glacier d'Argentière have allowed to establish a calibrated friction law that is observationally constrained and captures sliding velocity changes that occurred over the past decades (Gilbert et al., 2022). In this model, basal friction and subglacial hydrology are coupled through the transient evolution of the cavitation ratio θ as:

$$\tau_b^m = (1-\theta)\frac{U_b}{A_s} \tag{1}$$

where A_s is the Weertman friction coefficient (m a^{-1} MPa^{-m}), m is an exponent, and U_b is the basal sliding velocity. The evolution of θ through time is computed as a function of effective pressure N and sliding velocity U_b through the evolution equation of the form:

$$\frac{d\theta}{dt} = \frac{1}{l_r}\left(U_b(1-\theta)^{\frac{1}{q}} - A_s C^m |N|^{m-1} N \left(\frac{\theta}{\alpha}\right)^{\frac{1}{q}}\right) \tag{2}$$

where l_r is a characteristic length scale (m) representative of a distance between bedrock bumps, C, q, and α are positive constants as defined in (Gagliardini et al., 2007). Following (Gilbert et al., 2022), we solve the model in a slab configuration with geometry adapted to our study site, setting the basal slope to 3 degrees and τ_b equals 0.1 MPa as inferred from inversions of the basal condition (Gilbert et al., 2023). We use the same parameter values as constrained in (Togaibekov et al., 2024).

In this study, we apply the subglacial hydrological model proposed by (Gilbert et al., 2022), where hydrological transmissivity is derived from the cavitation state θ, as determined by the friction law in Equation 1. Both the water sheet thickness h (in meters) and the sheet conductivity k_s are expressed in relation to the variable θ with:

$$h = h_r \theta^{p_1} \tag{3}$$

$$k_s = k_0 \theta^{p_2} \tag{4}$$

where h_r denotes the average height of bedrock bumps (in meters), k_0 the intrinsic sheet conductivity, and p_1,p_2 are exponents.

3 Results

3.1 Temporal variations

3.1.1 Observed seasonal variations of glacier motion

We observe clear seasonal variations in both vertical and horizontal motion during the three-year monitoring period (Fig. 2). Surface horizontal velocity and vertical displacement begin to increase immediately after the melting season ends, typically

https://doi.org/10.5194/egusphere-2025-6293
Preprint. Discussion started: 23 January 2026

in October–November (Fig. 2a–c), coinciding with an increase in water pressure, as observed in winter 2019-2020 (Fig. 2b), reaching its peak close to overburden pressure around the highest velocity and uplift in May, known as the "spring event" (Iken and Bindschadler, 1986; Mair et al., 2003). The spring event occurs when the glacier is still snow-covered, immediately after the air temperature exceeds 0°C but shortly before the onset of the water discharge rise, and lasts for about five days (Fig. 2). Following this event, both horizontal velocity and vertical displacement start to decline early in the melting season, while water discharge remains elevated throughout the summer months, fluctuating between 5 $m^3\ s^{-1}$ and 15 $m^3\ s^{-1}$. While vertical displacement declines progressively, horizontal velocity exhibits short-term variations as long as water discharge is high (Fig. 2b). The minimum values of GPS-derived horizontal velocity and vertical displacement coincide with a significant drop in water discharge, typically in October–November, sometimes referred to in the literature as the "fall event" (Fudge et al., 2008; Rada and Schoof, 2018). The vertical velocity, on the other hand, is in anti-phase with water discharge, being negative during the summer months and positive from September to May. Similar behavior with smaller amplitude is also observed at station ARGG (Fig. S2), located approximately 3 km upstream, closer to the equilibrium line, suggesting that similar processes are at play in a significant portion of the glacier.

3.1.2 Comparison with the cavitometer velocities

The sliding velocity measured by the cavitometer in the icefall area (see Figure 1) differs from the GPS-recorded surface velocity in both magnitude and timing (Fig. 2b). The sliding velocity decreases toward a plateau over winter and increases significantly (up to approximately 25–30 m a^{-1}) as water discharge rises at the onset of melt in April. In contrast, the GPS-derived surface velocity increases progressively over winter, starting in November, by up to 15 m a^{-1}. During the melt period, the cavitometer shows velocity variations similar to those in the GPS records but with a different amplitude due to higher basal shear stress at the cavitometer location (Gilbert et al., 2022). The winter of 2020-2021 is characterized by the lowest sliding velocities at the cavitometer, around 30 m a^{-1}. Interestingly, this coincides with the smallest winter increase in GPS-derived surface velocity before the onset of the spring event, and it was preceded by the smallest velocity decrease in autumn (Fig. 2b). It is important to note that the water discharge level remains constant at about 1 $m^3\ s^{-1}$ throughout the winter, indicating that basal water circulates beneath the glacier year-round. The water discharge measurement system was upgraded in autumn 2020 because the previous system was not accurate enough to record low water discharge. This limitation explains the zero values observed during the winters of 2018–2019 and 2019–2020.

3.1.3 Comparison with modeled velocities

The hydro-mechanical model, originally developed based on cavitometer measurements, only partially reproduces the seasonal patterns of velocity and uplift observed by GPS (Fig. 2b). The main discrepancy is that the model underestimates both the observed winter speed-up and uplift, which were previously found to result from enhanced bed separation due to increased storage of basal water in isolated cavities (Vincent et al., 2022). If this is the case, the model cannot, by design, simulate rising winter water pressures in isolated hydraulic systems — a common limitation of current subglacial hydraulic models, which often fail to reproduce highly pressurized and disconnected subglacial environments (Hoffman et al., 2016; Flowers,

https://doi.org/10.5194/egusphere-2025-6293
Preprint. Discussion started: 23 January 2026

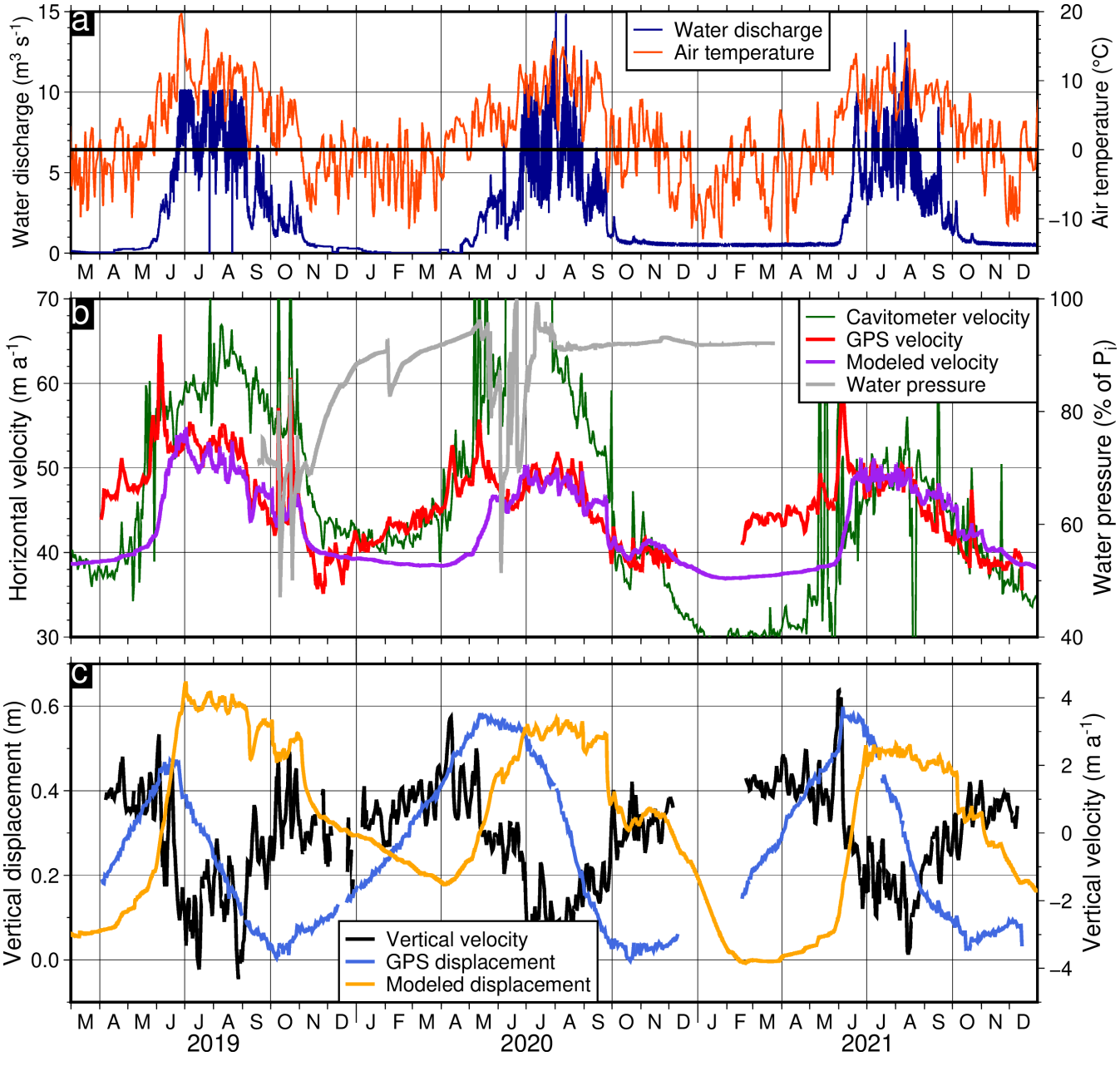

Figure 2. Seasonal variations in (a) water discharge and air temperature, (b) horizontal velocity and water pressure, and (c) vertical displacement and vertical velocity time series over a 3-year observational period from 2019 to 2021. The GPS-derived horizontal velocity, vertical displacement, and vertical velocity are given as an average across all available GPS sites. Water pressure is expressed as a percentage of the ice overburden pressure (p_i) for an ice thickness of 255 m.

https://doi.org/10.5194/egusphere-2025-6293
Preprint. Discussion started: 23 January 2026

2015). However, during the summer period, the model accurately captures horizontal velocity variations but also produces changes in cavity size that are different from the one inferred by GPS observation (Fig. 2c). These discrepancies between the measurements and the model raise the question of whether the observed summer subsidence is truly representative of bed separation or whether the model lacks the appropriate physics.

3.1.4 Temporal relationship between bed separation and horizontal velocity

The seasonal relationship between winter uplift and velocity speed-up is approximately linear ($\sim$27 m a^{-1} per meter of uplift) (Fig. 3a,b), although short-term variations in horizontal velocity appear to be uncorrelated with the observed uplift, as they are mainly driven by rapid changes in water pressure at a constant cavitation state (Togaibekov et al., 2024). Equations (1) and (3) provide a good order of magnitude for the relationship between winter speed-up and uplift (dark gray line in Fig. 3b), suggesting that bed uplift could serve as a good proxy for the overall cavitation state θ at the glacier base. This relationship is also valid at the end of summer, when water discharge significantly decreases (below 5 m^3 s^{-1}), typically from late August to early November (Fig. 3a,c). However, the horizontal velocity appears to be uncorrelated with bed separation during the subsidence phase right after the "spring event" in May. During periods of high water discharge, which usually encompass most of the summer months, cavities shrink at nearly constant horizontal velocity, possibly due to other processes affecting overall bed friction during this period. This deviation is less apparent in stake measurements, likely due to their lower temporal resolution (triangles and stars in Fig. 3c).

3.2 Spatial variations

3.2.1 Vertical displacement patterns

The spatial patterns of winter uplift (Fig. 4b,e) and summer subsidence (Fig. 5b,e) consistently occur at the same locations with comparable magnitude each year. For example, the GPS site AR3D on the right bank consistently records the largest uplift and subsidence. Uplift at site AR3D reaches almost 1 m during the longest observed period (winter 2020-2021) while the average uplift is about 0.5 m (Fig. 4e), and the lowest uplift of approximately 0.3 m occurs at site AR3G. We note that the period length is not consistent from year to year due to data gaps at certain stations, which limit the time window over which we have complete GPS network coverage. Overall, the spatial pattern of winter uplift observed in our study is consistent with that reported by Vincent et al. (2022) for the winter of 2019–2020 (Fig. S3).

3.2.2 Spatial relationship between bed separation and horizontal velocity

We compare the spatial patterns of winter uplift and summer subsidence with the average horizontal velocity and the horizontal velocity change (HVC), defined as the difference between the winter and summer extrema in the horizontal velocity time series (Fig.s 4 and 5). During summer, the spatial correlation between surface subsidence and summer HVC is not apparent. In contrast, we find that the spatial pattern of winter HVC closely matches the winter uplift pattern each year. For example, during the longest recorded winter period of 2020-2021, the highest HVC of over 4 m a^{-1} occurred at site AR3D, where the maximum

https://doi.org/10.5194/egusphere-2025-6293
Preprint. Discussion started: 23 January 2026

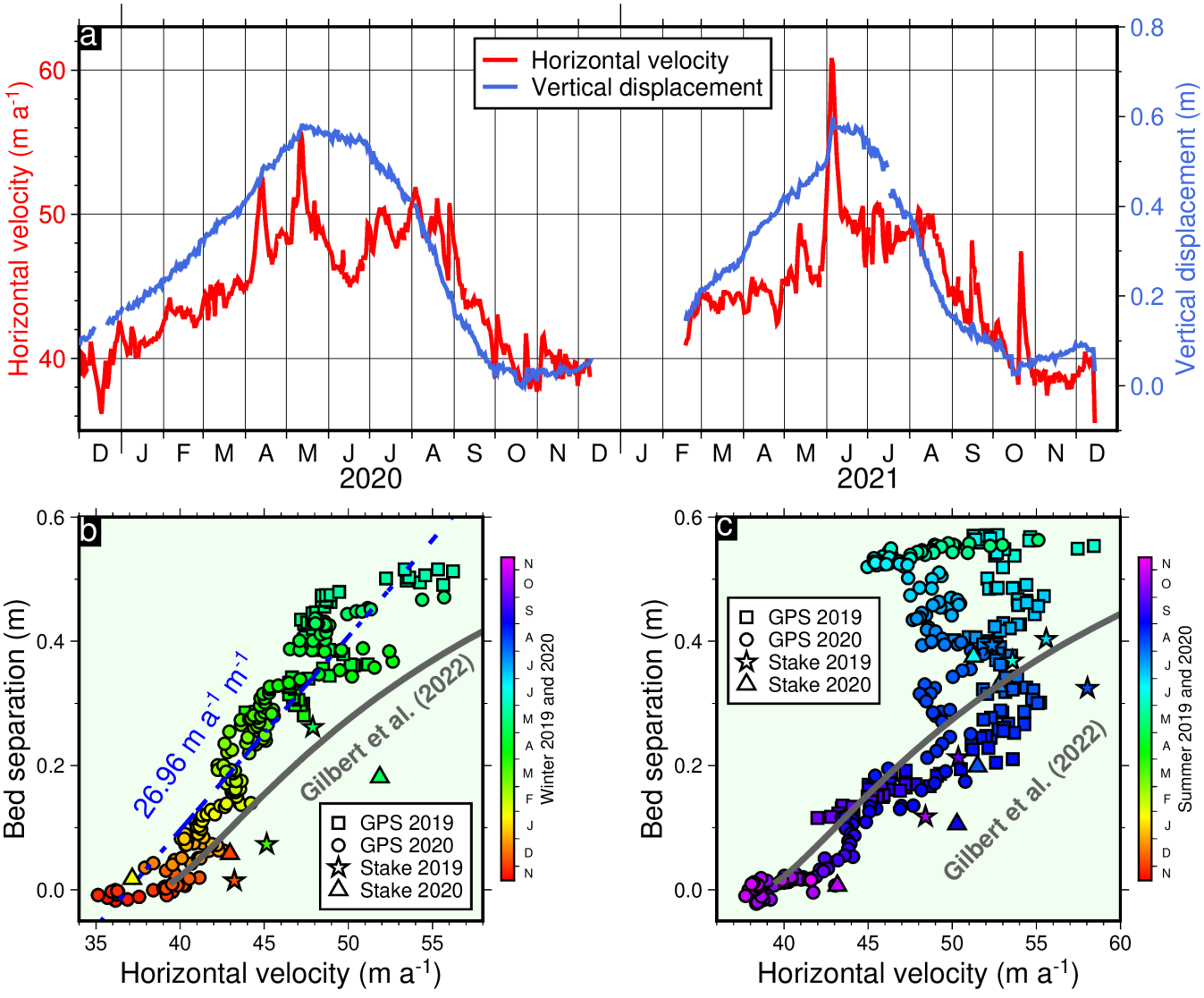

Figure 3. Relationship between bed separation and horizontal velocity during the melting seasons. (a) Time series of horizontal velocity and hydrologically induced vertical displacement (2020–2021), averaged over 12 GPS sites. (b) Relationship between temporal changes (spatially averaged over 12 GPS sites) in horizontal velocity and bed separation in (b) winters and (c) summers 2018-2020, with ablation stake measurements in 2018-2020 (Vincent et al., 2022, Fig. 9c). Slope of a linear fit in (b) is given only over GPS measurements.

https://doi.org/10.5194/egusphere-2025-6293
Preprint. Discussion started: 23 January 2026

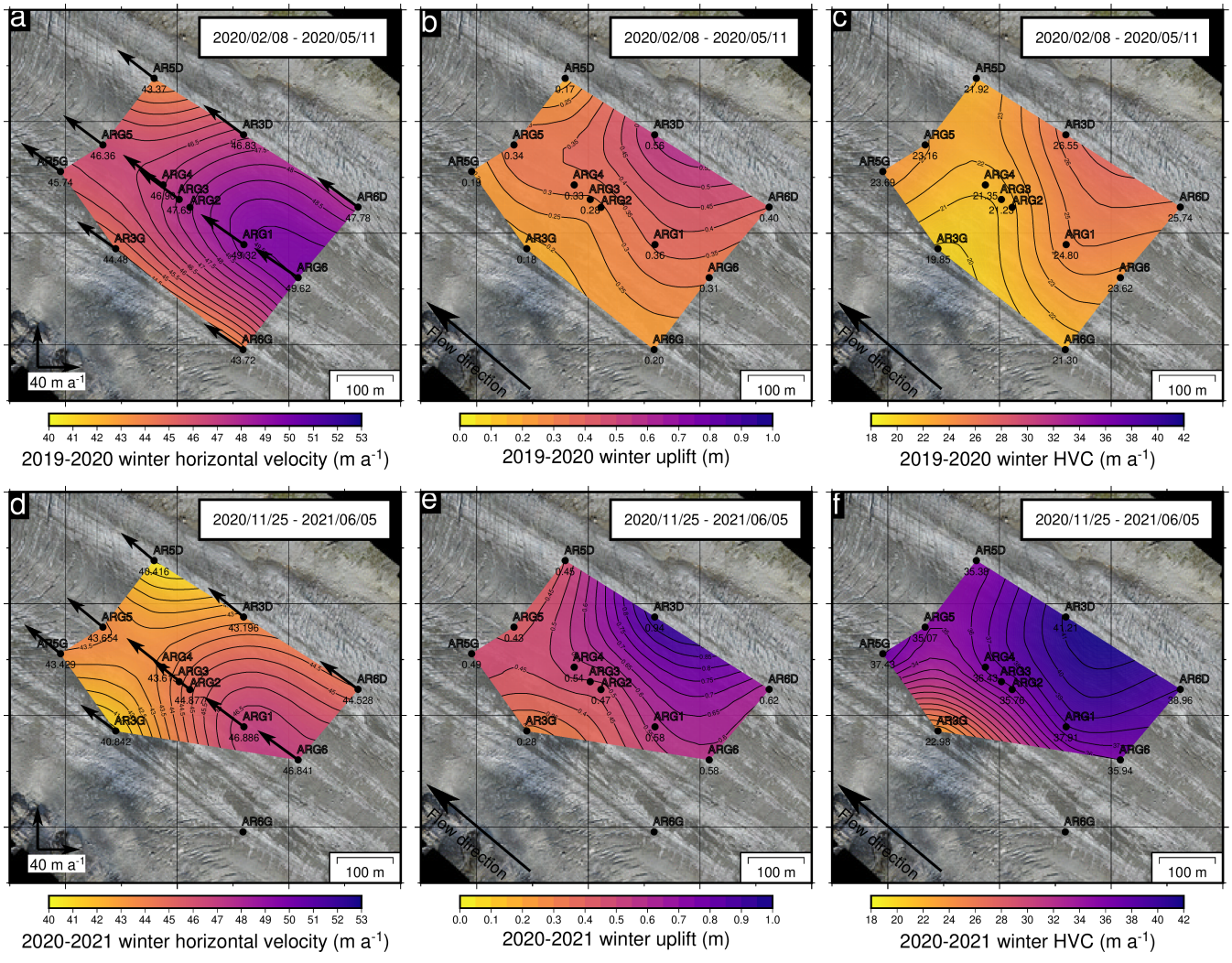

Figure 4. Spatial pattern of (a,d) average horizontal velocity, (b,e) vertical displacement, and (c,f) horizontal velocity change in winter 2020 (top panels) and 2020/2021 (bottom panels).

uplift was observed. We also observe a decreasing gradient toward the left bank in both uplift and HVC, where HVC dropped to approximately 2–3 m a^{-1} at site AR3G, which is almost half the value observed at AR3D (Fig. 4). The reason why the cavities are larger on the right bank remains unclear, but it may be related to the heavily crevassed terrain, which could favor local water storage that is then slowly released during the winter months.

3.2.3 Spatial and temporal consistency between bed separation and horizontal velocity

Similar to the temporal analysis of the relationship between bed separation and horizontal velocity (Fig. 3b–c), we examine this relationship in space across 12 GPS stations during the winters (Fig. 6a) and summers (Fig. 6b) between 2020 and 2021.

https://doi.org/10.5194/egusphere-2025-6293
Preprint. Discussion started: 23 January 2026

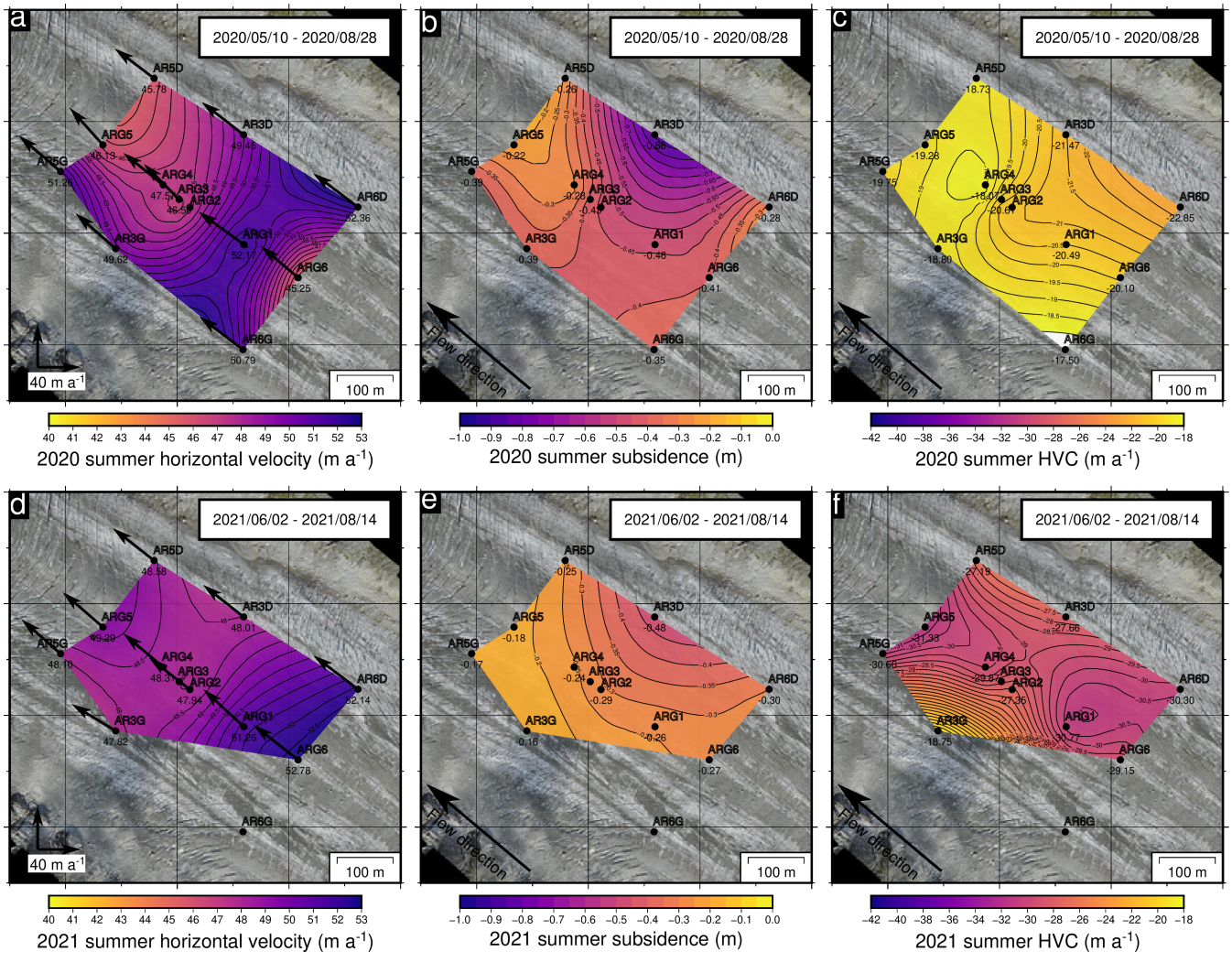

Figure 5. Spatial pattern of (a,d) horizontal velocity, (b,e) vertical displacement, and (c,f) horizontal velocity change in summer 2020 (top panels) and 2021 (bottom panels).

https://doi.org/10.5194/egusphere-2025-6293
Preprint. Discussion started: 23 January 2026

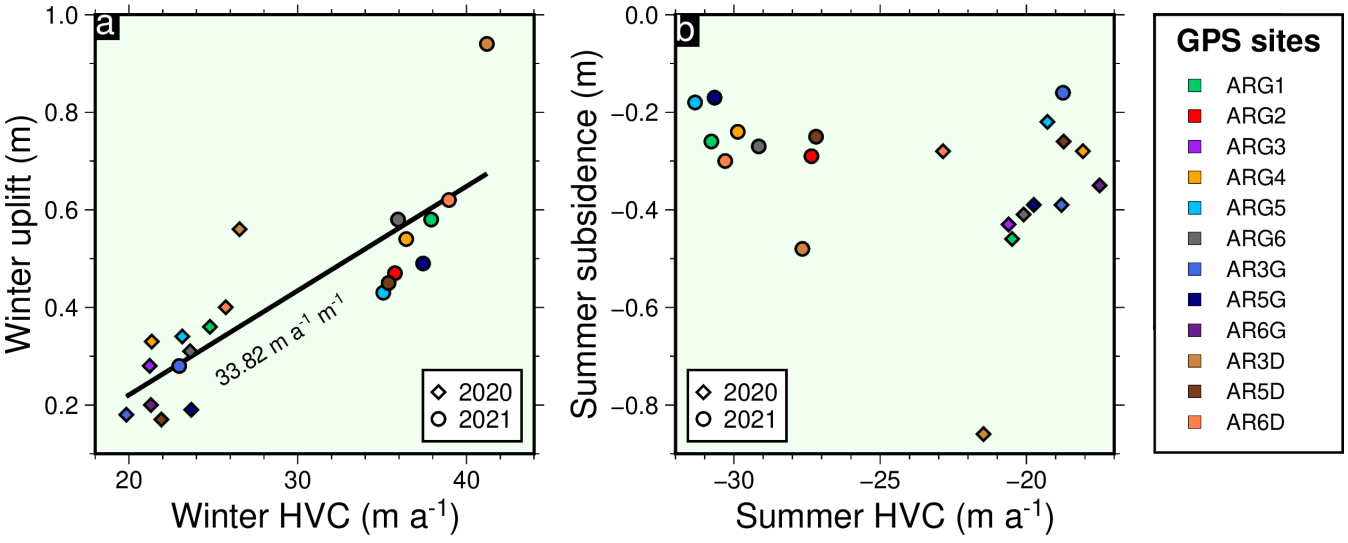

Figure 6. Spatial relationship between bed separation and horizontal velocity over 12 GPS sites averaged (a) winters and (b) summers 2020-2021.

We find that the spatial relationship between winter uplift and HVC across these stations is approximately 34 m a^{-1} per meter of uplift, which is remarkably similar to the temporal relationship over the same period ($\sim$27 m a^{-1} m^{-1}). This is a strong evidence that changes in cavity dynamics during winter control both the spatial and temporal variations in surface velocities. This relationship, just like in temporal analysis, is less evident in summer (Fig. 6b), suggesting that additional factors influence glacier velocity during that season. We also observe that the spatial patterns of HVC vary from year to year (Fig. 5c,f), whereas the subsidence pattern remains more consistent (Fig. 5b,e).

4 Discussion

4.1 Winter acceleration

To assess the total contribution of bed separation to the observed surface uplift, we first examine whether the vertical displacements measured during winter could be affected by spatial variations in strain rate (Text S1). To do this, we estimate the winter strain rate anomaly relative to the annual mean by computing the evolution of the surface velocity gradient (Fig. S4). We find that the spatial pattern of the strain rate anomaly does not match that of the observed vertical displacement, suggesting that changes in strain rate cannot explain the observed uplift. A similar conclusion was reached by Vincent et al. (2022) using a three-dimensional ice-flow model. We note that integrating the strain rate over the glacier depth, assuming it is homogeneous with depth, and over the considered time periods results in a vertical displacement magnitude greater than the observed uplift (Fig. S5). This likely indicates that the assumption of depth-homogeneous strain rate is not valid (Sugiyama and Gudmundsson, 2004); however, future measurements of internal vertical strain in boreholes are needed to observationally confirm this.

https://doi.org/10.5194/egusphere-2025-6293
Preprint. Discussion started: 23 January 2026

The variations in both horizontal velocity and vertical displacement observed at all GPS sites suggest that, in winter, the glacier decouples from its bed across a large area. The concurrent increase in water pressure indicates that the uplift is associated with the growth of basal cavities in response to rising water pressure. Given the limited amount of water available in winter, the increasing pressure must originate from the subglacial hydraulic network becoming inefficient as it transitions into a system of largely disconnected cavities. The winter water likely results from basal melt driven by frictional heating, geothermal flux, and/or the release of residual englacial water from the previous ablation season (Harper et al., 2005; Ryser et al., 2014; Sommers et al., 2023). The presence of liquid water beneath the glacier is further supported by the observed winter discharge of approximately 1 m^3 s^{-1}, detected after the measurement device was upgraded in autumn 2020 (Fig. 2a).

Vertical subsidence concomitant with the onset of melt suggests that cavities connect in response to meltwater input, indicating that a minimum amount of extra subglacial discharge from surface melt is required the transition and maintenance of a connected cavity network. This suggests that, at this site, cavities cannot connect mechanically (i.e., through growth driven by increased water pressure and sliding speed), but instead require flowing water forming channel-like conduits to establish connections. Interestingly, winter acceleration is not detected at the cavitometer, which is located a few hundred meters from the GPS sites. We suggest that these differences may result from different hydraulic potential gradients caused by drastically different surface slopes at the two locations (approximately 10 % at the GPS sites and 25 % at the cavitometer). The higher hydraulic potential gradient at the cavitometer may facilitate hydraulic connections at lower water pressures in winter, thereby preventing cavity growth and the associated acceleration of sliding. This explanation would be consistent with the channel-like control on effective pressure proposed by Gimbert et al. (2021a) to explain constant winter effective pressure over multi-decadal timescales in this steeper part of the glacier.

4.2 Surface velocity variations during the melt season

Water pressure starts declining after the spring acceleration (Fig. 2b), consistent with the subglacial drainage system transitioning from inefficient to efficient (Iken and Bindschadler, 1986). From this point onward, velocity variations are well captured by the hydro-mechanical model representing connected cavity dynamics (Fig. 2b), consistent with the glacier entering a regime where water pressure is regulated by coupled cavity dynamics and drainage that directly evolve in response to changes in water input (Gilbert et al., 2022). However, during the high melting period (June–July), the observed vertical displacement (subsidence) no longer matches the observed velocities, which remain nearly constant despite surface subsidence (Fig. 3c). This lack of correlation between surface velocity change and surface subsidence also holds spatially, as the summer spatial subsidence pattern does not match the summer spatial velocity change pattern (Fig.s 5 and 6). This suggests that subglacial cavity size is not the only factor controlling sliding velocity at this time of year. Unsteady friction driven by short-term pulses in water pressure caused by large fluctuations in water discharge could explain this deviation (Rada and Schoof, 2018; Fudge et al., 2008; Sugiyama and Gudmundsson, 2004), since, in that case, local short-term increases in water pressure are expected to instantaneously increase the overall sliding speed (Togaibekov et al., 2024), despite average pressure progressively decreasing and thus cavities progressively closing. Later in the season (August–September), velocity changes become again correlated with surface subsidence (Fig. 3c), indicating that they primarily control the sliding velocities at this time. The spatial pattern

https://doi.org/10.5194/egusphere-2025-6293
Preprint. Discussion started: 23 January 2026

of summer subsidence also matches fairly well that of winter uplift (Fig.s 4 and 5), which is consistent with cavities closing in summer being the same as those opening in winter.

4.3 General implications

A similar monotonic increase in winter surface velocities has previously been observed in many Greenland outlet glaciers (Sole et al., 2013; Moon et al., 2014), where it was attributed to a steady wintertime rise in basal water pressure of up to 20 %, driven primarily by basal meltwater generated from sliding-induced friction (Harper et al., 2021). This water is thought to circulate through a weakly connected network of subglacial cavities (Hoffman et al., 2016), highlighting a hydrology–dynamics coupling that aligns with our findings at Argentière Glacier. Our observations confirm this mechanism by showing that winter acceleration results from growing cavities becoming isolated (Sole et al., 2013).

Interestingly, we find that the typical seasonal dynamics observed under the low surface slope at our GPS site are no longer present a few hundred meters downglacier, where cavitometer measurements are made under a much steeper glacier surface slope. This suggests that geometrical factors such as surface slope may control subglacial hydraulic conditions. This influence of surface slope has been proposed to play a key role in the long-term response of glacier velocity to thickness changes (Maier et al., 2022) and could also exert a primary control on glacier seasonal dynamics.

5 Conclusions

We monitored the seasonal horizontal and vertical motions in the ablation zone of Glacier d'Argentière using a dense network of GPS stations over a three-year period. By combining these measurements with complementary observations of water pressure, water discharge, and sliding velocity, together with a coupled hydro-mechanical model, we characterize two distinct alternating seasonal phases, referred to here as the winter and summer periods. We show that the glacier progressively accelerates and uplifts throughout winter as observed in a few studies from Greenland (Sole et al., 2013; Moon et al., 2014) but rarely on mountain glaciers (Vincent et al., 2022). Our results provide strong evidence that the observed surface uplift reflects variations in bed separation, which drives frictional change throughout winter. This is evident from the clear temporal and spatial relationships between bed separation and the increase in horizontal velocity ($\sim$ 30 m a^{-1} per meter of uplift), which follow model prediction of Gilbert et al. (2022). This indicates that winter acceleration is driven by the growth of highly pressurized cavities as subglacial water pressure rises through winter and approaches the overburden pressure near the "spring event". The sustained high water pressure in the absence of water input from the surface suggests that the cavities are weakly connected, as observed in Greenland (Hoffman et al., 2016).

During the two first months of the melt period, the relationship between bed separation and horizontal velocity no longer holds and cavity shrinkage becomes uncorrelated with glacier deceleration, both temporally and spatially, suggesting that processes other than subglacial cavitation may also influence sliding speed. We attribute this lack of correlation to unsteady cavity dynamics driven by highly variable short-term water pressure in response to large fluctuations in water discharge, a

https://doi.org/10.5194/egusphere-2025-6293
Preprint. Discussion started: 23 January 2026

phenomenon previously observed in many glaciers, including Glacier d'Argentière. Later in the summer, however, the decrease in velocity again becomes related to surface subsidence associated with the closure of subglacial cavities.

These two phases result in a seasonal cycle characterized by peak velocity at the end of winter and a general decrease in velocity during the summer months. This contrasts with observations made at the nearby Argentière cavitometer, where the seasonal cycle is directly correlated with melt discharge Gilbert et al. (2022). It shows that local effects can influence how the different hydrological components of the subglacial drainage system control the effective pressure throughout the year. In particular, the existence of weakly connected, high-pressure cavities that grow in winter appears to be limited to certain areas. These observations can be directly linked to the different types of seasonal variability of types II and III observed in Greenland Moon et al. (2014). Our study sheds light on the various seasonal velocity patterns by providing detailed insights into the factors driving the sliding velocity throughout the year.

Data availability

The GPS data used in this study are archived on the Oreme repository (Walpersdorf et al., 2023a, b, c). Other data can be accessed through the Zenodo repository available (Togaibekov et al., 2023; Togaibekov, 2025; Vincent, 2021).

Author contributions

All authors contributed to the conceptualization of the work. AT and AW maintained the GPS network and processed the GPS data. FG and AW supervised the work and provided funding. AG designed and performed the numerical simulations. AT analyzed the data, and all authors interpreted the results. AT lead the writing of the manuscript, with inputs from all co-authors.

Competing interests

The authors declare no competing interests.

Acknowledgments

This work is part of the SAUSSURE project (ANR-18-CE01-0015-01) supported by the French National Research Agency (ANR). The GPS equipment was provided by the French national mobile parc GPSmob. We thank all the people who conducted fieldwork, particularly Laurent Ott, Agnès Helmstetter, Christian Sue, and Martin Champon. We thank Luc Moreau for providing cavitometer data, and Luc Piard for conducting the drilling operations.

https://doi.org/10.5194/egusphere-2025-6293
Preprint. Discussion started: 23 January 2026

References

Anderson, R. S., Anderson, S. P., MacGregor, K. R., Waddington, E. D., O'Neel, S., Riihimaki, C. A., and Loso, M. G.: Strong feedbacks between hydrology and sliding of a small alpine glacier, J. Geophys. Res. Earth Surf., 109, https://doi.org/10.1029/2004JF000120, 2004.

Andrews, L. C., Catania, G. A., Hoffman, M. J., Gulley, J. D., Lüthi, M. P., Ryser, C., Hawley, R. L., and Neumann, T. A.: Direct observations of evolving subglacial drainage beneath the Greenland Ice Sheet, Nature, 514, 80–83, https://doi.org/10.1038/nature13796, 2014.

Bartholomaus, T. C., Anderson, R. S., and Anderson, S. P.: Growth and collapse of the distributed subglacial hydrologic system of Kennicott Glacier, Alaska, USA, and its effects on basal motion, J. Glaciol., 57, 985–1002, https://doi.org/10.3189/002214311798843269, 2011.

Bingham, R. G., Hubbard, A. L., Nienow, P. W., and Sharp, M. J.: An investigation into the mechanisms controlling seasonal speedup events at a High Arctic glacier, Journal of Geophysical Research: Earth Surface, 113, https://doi.org/10.1029/2007JF000832, _eprint: https://onlinelibrary.wiley.com/doi/pdf/10.1029/2007JF000832, 2008.

Bock, Y., Gourevitch, S. A., Counselman, III, C. C., King, R. W., and Abbot, R. I.: Interferometric analysis of GPS phase observations, Manuscr. Geodaet., 11, 282–288, 1986.

Davison, B. J., Sole, A. J., Livingstone, S. J., Cowton, T. R., and Nienow, P. W.: The Influence of Hydrology on the Dynamics of Land-Terminating Sectors of the Greenland Ice Sheet, Front. Earth Sci., 7, https://doi.org/10.3389/feart.2019.00010, 2019.

Flowers, G. E.: Modelling water flow under glaciers and ice sheets, Proc. R. Soc. A, 471, 20140 907, https://doi.org/10.1098/rspa.2014.0907, 2015.

Fountain, A. G. and Walder, J. S.: Water flow through temperate glaciers, Rev. Geophys., 36, 299–328, 1998.

Fowler, A. C.: Sliding with Cavity Formation, Journal of Glaciology, 33, 255–267, https://doi.org/10.3189/S0022143000008820, publisher: Cambridge University Press, 1987.

Fudge, T. J., Humphrey, N. F., Harper, J. T., and Pfeffer, W. T.: Diurnal fluctuations in borehole water levels: configuration of the drainage system beneath Bench Glacier, Alaska, USA, J. Glaciol., 54, 297–306, https://doi.org/10.3189/002214308784886072, 2008.

Gagliardini, O., Cohen, D., Råback, P., and Zwinger, T.: Finite-element modeling of subglacial cavities and related friction law, Journal of Geophysical Research: Earth Surface, 112, https://doi.org/10.1029/2006JF000576, 2007.

Gilbert, A., Gimbert, F., Thøgersen, K., Schuler, T. V., and Kääb, A.: A Consistent Framework for Coupling Basal Friction With Subglacial Hydrology on Hard-Bedded Glaciers, Geophys. Res. Lett., 49, e2021GL097 507, https://doi.org/10.1029/2021GL097507, 2022.

Gilbert, A., Gimbert, F., Gagliardini, O., and Vincent, C.: Inferring the Basal Friction Law From Long Term Changes of Glacier Length, Thickness and Velocity on an Alpine Glacier, Geophys. Res. Lett., 50, e2023GL104 503, https://doi.org/10.1029/2023GL104503, 2023.

Gimbert, F., Gilbert, A., Gagliardini, O., Vincent, C., and Moreau, L.: Do Existing Theories Explain Seasonal to Multi-Decadal Changes in Glacier Basal Sliding Speed?, Geophysical Research Letters, 48, e2021GL092 858, https://doi.org/10.1029/2021GL092858, 2021a.

Gimbert, F., Nanni, U., Roux, P., Helmstetter, A., Garambois, S., Lecointre, A., Walpersdorf, A., Jourdain, B., Langlais, M., Laarman, O., Lindner, F., Sergeant, A., Vincent, C., and Walter, F.: A Multi-Physics Experiment with a Temporary Dense Seismic Array on the Argentière Glacier, French Alps: The RESOLVE Project, Seismol. Res. Lett., 92, 1185–1201, https://doi.org/10.1785/0220200280, 2021b.

Gordon, S., Sharp, M., Hubbard, B., Smart, C., Ketterling, B., and Willis, I.: Seasonal reorganization of subglacial drainage inferred from measurements in boreholes, Hydrol. Process., 12, 105–133, https://doi.org/10.1002/(SICI)1099-1085(199801)12:1<105::AID-HYP566>3.0.CO;2-#, 1998.

Hantz, D. and Lliboutry, L.: Waterways, Ice Permeability at Depth, and Water Pressures at Glacier D'Argentière, French Alps, Journal of Glaciology, 29, 227–239, https://doi.org/10.3189/S0022143000008285, publisher: Cambridge University Press, 1983.

https://doi.org/10.5194/egusphere-2025-6293
Preprint. Discussion started: 23 January 2026

Harper, J., Meierbachtol, T., Humphrey, N., Saito, J., and Stansberry, A.: Generation and fate of basal meltwater during winter, western Greenland Ice Sheet, Cryosphere, 15, 5409–5421, https://doi.org/10.5194/tc-15-5409-2021, 2021.

Harper, J. T., Humphrey, N. F., Pfeffer, W. T., Fudge, T., and O'Neel, S.: Evolution of subglacial water pressure along a glacier's length, Ann. Glaciol., 40, 31–36, https://doi.org/10.3189/172756405781813573, 2005.

Herring, T. A., King, R. W., Floyd, M. A., and McClusky, S. C.: Introduction to GAMIT/GLOBK, 2018.

Hewitt, I. J., Schoof, C., and Werder, M. A.: Flotation and free surface flow in a model for subglacial drainage. Part 2. Channel flow, J. Fluid Mech., 702, 157–187, https://doi.org/10.1017/jfm.2012.166, 2012.

Hodge, S. M.: Variations in the Sliding of a Temperate Glacier, J. Glac., 13, 349–369, https://doi.org/10.3189/S0022143000023157, 1974.

Hoffman, M. J., Andrews, L. C., Price, S. F., Catania, G. A., Neumann, T. A., Lüthi, M. P., Gulley, J., Ryser, C., Hawley, R. L., and Morriss, B.: Greenland subglacial drainage evolution regulated by weakly connected regions of the bed, Nat. Commun., 7, 13 903, https://doi.org/10.1038/ncomms13903, 2016.

Iken, A.: The Effect of the Subglacial Water Pressure on the Sliding Velocity of a Glacier in an Idealized Numerical Model, J. Glaciol., 27, 407–421, https://doi.org/10.3189/S0022143000011448, 1981.

Iken, A. and Bindschadler, R. A.: Combined measurements of Subglacial Water Pressure and Surface Velocity of Findelengletscher, Switzerland: Conclusions about Drainage System and Sliding Mechanism, J. Glaciol., 32, 101–119, https://doi.org/10.3189/S0022143000006936, 1986.

Iken, A., Röthlisberger, H., Flotron, A., and Haeberli, W.: The Uplift of Unteraargletscher at the Beginning of the Melt Season—A Consequence of Water Storage at the Bed?, J. Glaciol., 29, 28–47, https://doi.org/10.3189/S0022143000005128, 1983.

Kamb, B.: Sliding motion of glaciers: Theory and observation, Reviews of Geophysics, 8, 673–728, https://doi.org/10.1029/RG008i004p00673, _eprint: https://onlinelibrary.wiley.com/doi/pdf/10.1029/RG008i004p00673, 1970.

Kamb, B.: Glacier surge mechanism based on linked cavity configuration of the basal water conduit system, J. Geophys. Res. Solid Earth, 92, 9083–9100, https://doi.org/10.1029/JB092iB09p09083, 1987.

King, M.: Rigorous GPS data-processing strategies for glaciological applications, J. Glac., 50, 601–607, https://doi.org/10.3189/172756504781829747, 2004.

Lliboutry, L.: Contribution a la theorie du frottement du glacier sur son lit, Comptes Rendus Hebdomadaires des Seances de l'Academie des Sciences, 247, 318–320, 1958.

Lliboutry, L.: General Theory of Subglacial Cavitation and Sliding of Temperate Glaciers, J. Glac., 7, 21–58, https://doi.org/10.3189/S0022143000020396, 1968.

Maier, N., Gimbert, F., and Gillet-Chaulet, F.: Threshold response to melt drives large-scale bed weakening in Greenland, Nature, 607, 714–720, https://doi.org/10.1038/s41586-022-04927-3, 2022.

Mair, D., Nienow, P., Willis, I., and Sharp, M.: Spatial patterns of glacier motion during a high-velocity event: Haut Glacier d'Arolla, Switzerland, J. Glac., 47, 9–20, https://doi.org/10.3189/172756501781832412, 2001.

Mair, D., Willis, I., Fischer, U. H., Hubbard, B., Nienow, P., and Hubbard, A.: Hydrological controls on patterns of surface, internal and basal motion during three "spring events": Haut Glacier d'Arolla, Switzerland, J. Glac., 49, 555–567, https://doi.org/10.3189/172756503781830467, 2003.

Moon, T., Joughin, I., Smith, B., van den Broeke, M. R., van de Berg, W. J., Noël, B., and Usher, M.: Distinct patterns of seasonal Greenland glacier velocity, Geophys. Res. Lett., 41, 7209–7216, https://doi.org/10.1002/2014GL061836, 2014.

https://doi.org/10.5194/egusphere-2025-6293
Preprint. Discussion started: 23 January 2026

Nanni, U., Gimbert, F., Vincent, C., Gräff, D., Walter, F., Piard, L., and Moreau, L.: Quantification of seasonal and diurnal dynamics of subglacial channels using seismic observations on an Alpine glacier, Cryosphere, 14, 1475–1496, https://doi.org/10.5194/tc-14-1475-2020, 2020.

Nanni, U., Gimbert, F., Roux, P., and Lecointre, A.: Observing the subglacial hydrology network and its dynamics with a dense seismic array, Proc. Natl. Acad. Sci. U.S.A., 118, e2023757 118, https://doi.org/10.1073/pnas.2023757118, 2021.

Nienow, P., Sharp, M., and Willis, I.: Seasonal changes in the morphology of the subglacial drainage system, Haut Glacier d'Arolla, Switzerland, Earth Surf. Process. Landforms, 23, 825–843, https://doi.org/10.1002/(SICI)1096-9837(199809)23:9<825::AID-ESP893>3.0.CO;2-2, 1998.

Rada, C. and Schoof, C.: Channelized, distributed, and disconnected: subglacial drainage under a valley glacier in the Yukon, Cryosphere, 12, 2609–2636, https://doi.org/10.5194/tc-12-2609-2018, 2018.

Raymond, C. F., Benedict, R. J., Harrison, W. D., Echelmeyer, K. A., and Sturm, M.: Hydrological discharges and motion of Fels and Black Rapids Glaciers, Alaska, U.S.A.: implications for the structure of their drainage systems, J. Glac., 41, 290–304, https://doi.org/10.3189/S002214300001618X, 1995.

Ritz, C., Edwards, T. L., Durand, G., Payne, A. J., Peyaud, V., and Hindmarsh, R. C. A.: Potential sea-level rise from Antarctic ice-sheet instability constrained by observations, Nature, 528, 115–118, https://doi.org/10.1038/nature16147, 2015.

Roldán-Blasco, J.-P., Gilbert, A., Piard, L., Gimbert, F., Vincent, C., Gagliardini, O., Togaibekov, A., Walpersdorf, A., and Maier, N.: Creep enhancement and sliding in a temperate, hard-bedded alpine glacier, EGUsphere, pp. 1–25, https://doi.org/10.5194/egusphere-2024-1600, 2024.

Ryser, C., Lüthi, M. P., Andrews, L. C., Hoffman, M. J., Catania, G. A., Hawley, R. L., Neumann, T. A., and Kristensen, S. S.: Sustained high basal motion of the Greenland ice sheet revealed by borehole deformation, J. Glac., 60, 647–660, https://doi.org/10.3189/2014JoG13J196, 2014.

Röthlisberger, H.: Water Pressure in Intra- and Subglacial Channels, Journal of Glaciology, 11, 177–203, https://doi.org/10.3189/S0022143000022188, publisher: Cambridge University Press, 1972.

Schoof, C.: The effect of cavitation on glacier sliding, Proc. R. Soc. A, 461, 609–627, https://doi.org/10.1098/rspa.2004.1350, 2005.

Schoof, C.: Coulomb friction and other sliding laws in a higher-order glacier flow model, Math. Models Methods Appl. Sci., 20, 157–189, https://doi.org/10.1142/S0218202510004180, 2010.

Sole, A., Nienow, P., Bartholomew, I., Mair, D., Cowton, T., Tedstone, A., and King, M. A.: Winter motion mediates dynamic response of the Greenland Ice Sheet to warmer summers, Geophysical Research Letters, 40, 3940–3944, https://doi.org/10.1002/grl.50764, _eprint: https://onlinelibrary.wiley.com/doi/pdf/10.1002/grl.50764, 2013.

Sommers, A., Meyer, C., Morlighem, M., Rajaram, H., Poinar, K., Chu, W., and Mejia, J.: Subglacial hydrology modeling predicts high winter water pressure and spatially variable transmissivity at Helheim Glacier, Greenland, J. Glac., pp. 1–13, https://doi.org/10.1017/jog.2023.39, 2023.

Sugiyama, S. and Gudmundsson, G. H.: Short-term variations in glacier flow controlled by subglacial water pressure at Lauteraargletscher, Bernese Alps, Switzerland, J. Glac., 50, 353–362, https://doi.org/10.3189/172756504781829846, 2004.

Togaibekov, A.: SmartStake SMB, air temperature, snow depth measurements at Argentière Glacier between 2019 and 2021, https://doi.org/10.5281/zenodo.15023211, 2025.

Togaibekov, A., Gimbert, F., Gilbert, A., and Walpersdorf, A.: Sliding velocity, water discharge, water pressure, and rainfall time series at Argentière Glacier between 2019 and 2021, https://doi.org/10.5281/zenodo.10419097, 2023.

https://doi.org/10.5194/egusphere-2025-6293
Preprint. Discussion started: 23 January 2026

Togaibekov, A., Gimbert, F., Gilbert, A., and Walpersdorf, A.: Observing and Modeling Short-Term Changes in Basal Friction During Rain-Induced Speed-Ups on an Alpine Glacier, Geophys. Res. Lett., 51, e2023GL107 999, https://doi.org/10.1029/2023GL107999, 2024.

Togaibekov, A., Gimbert, F., Rabatel, A., and Walpersdorf, A.: Surface mass balance monitoring of an alpine glacier using GNSS Interferometric Reflectometry, J. Glac., 71, e111, https://doi.org/10.1017/jog.2025.10086, 2025.

Vernay, M., Lafaysse, M., Monteiro, D., Hagenmuller, P., Nheili, R., Samacoïts, R., Verfaillie, D., and Morin, S.: The S2M meteorological and snow cover reanalysis over the French mountainous areas: description and evaluation (1958–2021), Earth Syst. Sci. Data, 14, 1707–1733, https://doi.org/10.5194/essd-14-1707-2022, 2022.

Vincent, C.: Ice flow velocities and uplift, https://doi.org/10.5281/zenodo.5536953, 2021.

Vincent, C. and Moreau, L.: Sliding velocity fluctuations and subglacial hydrology over the last two decades on Argentière glacier, Mont Blanc area, J. Glaciol., 62, 805–815, https://doi.org/10.1017/jog.2016.35, 2016.

Vincent, C., Soruco, A., Six, D., and Meur, E. L.: Glacier thickening and decay analysis from 50 years of glaciological observations performed on Glacier d'Argentière, Mont Blanc area, France, Ann. Glaciol.y, 50, 73–79, https://doi.org/10.3189/172756409787769500, 2009.

Vincent, C., Gilbert, A., Walpersdorf, A., Gimbert, F., Gagliardini, O., Jourdain, B., Roldan Blasco, J. P., Laarman, O., Piard, L., Six, D., Moreau, L., Cusicanqui, D., and Thibert, E.: Evidence of Seasonal Uplift in the Argentière Glacier (Mont Blanc Area, France), J. Geophys. Res. Earth Surf., 127, e2021JF006 454, https://doi.org/10.1029/2021JF006454, 2022.

Vivian, R. and Bocquet, G.: Subglacial Cavitation Phenomena Under the Glacier D'Argentière, Mont Blanc, France, J. Glac., 12, 439–451, https://doi.org/10.3189/S0022143000031853, 1973.

Walpersdorf, A., Ott, L., Helmstetter, A., Sue, C., Bouvier, J.-N., Champon, M., Moreau, L., Togaibekov, A., Gimbert, F., Six, D., Vincent, C., Garambois, S., Mercier, S., Laarman, O., Piard, L., Nanni, U., Mathey, M., Urruty, B., Romeyer, O., and Radiguet, M.: Epos-France - GPSMob data - Mission n° 19-050 - Argentiere (2019) - 2019-04-02 / 2020-01-01 - 7 points, https://doi.org/10.15148/744BE716-3207-4A26-BF7B-60B5FD304FFD, 2023a.

Walpersdorf, A., Ott, L., Helmstetter, A., Sue, C., Bouvier, J.-N., Champon, M., Moreau, L., Togaibekov, A., Gimbert, F., Six, D., Vincent, C., Garambois, S., Mercier, S., Laarman, O., Piard, L., Nanni, U., Mathey, M., Urruty, B., Romeyer, O., and Radiguet, M.: Epos-France - GPSMob data - Mission n° 20-021 - Argentiere (2020) - 2020-01-02 / 2021-01-01 - 13 points, https://doi.org/10.15148/3FD58616-E0C4-4A7F-B2A9-7CF3DB4933BA, 2023b.

Walpersdorf, A., Ott, L., Helmstetter, A., Sue, C., Bouvier, J.-N., Champon, M., Moreau, L., Togaibekov, A., Gimbert, F., Six, D., Vincent, C., Garambois, S., Mercier, S., Laarman, O., Piard, L., Nanni, U., Mathey, M., Urruty, B., Romeyer, O., and Radiguet, M.: Epos-France - GPSMob data - Mission n° 21-028 - Argentiere (2021) - 2021-01-02 / 2021-12-31 - 13 points, https://doi.org/10.15148/FF97D3BB-0DB2-4D21-8ABE-999A7C2565CD, 2023c.

Weertman, J.: On the Sliding of Glaciers, J. Glac., 3, 33–38, https://doi.org/10.3189/S0022143000024709, 1957.

Werder, M. A., Hewitt, I. J., Schoof, C. G., and Flowers, G. E.: Modeling channelized and distributed subglacial drainage in two dimensions, J. Geophys. Res. Earth Surf., 118, 2140–2158, https://doi.org/10.1002/jgrf.20146, 2013.

Zoet, L. K. and Iverson, N. R.: A slip law for glaciers on deformable beds, Science, 368, 76–78, https://doi.org/10.1126/science.aaz1183, 2020.